

Deriving super-horizon curvature perturbations from the dynamics of preheating

Arindam Mazumdar,^a Kamakshya Prasad Modak^b

^aTheory Division, Saha Institute of Nuclear Physics, Kolkata-64, India

^bAstroparticle Physics and Cosmology Division, Saha Institute of Nuclear Physics, Kolkata-64, India

E-mail: arindam.mazumdar@saha.ac.in, kamakshya.modak@saha.ac.in

Abstract. We present a framework for calculating super-horizon curvature perturbation from the dynamics of preheating, which gives a reasonable match to the lattice results. Hubble patches with different initial background field values evolve differently. From the bifurcation of their evolution trajectories we find curvature perturbation using Lyapunov theorem and δN formulation. In this way we have established a connection between the finer dynamics of preheating and the curvature perturbation produced in this era. From the calculated analytical form of the curvature perturbation we have derived the effective super-horizon curvature perturbation smoothed out on large scales of CMB. The order of the amount of local form non-gaussianity generated in this process has been calculated and problems regarding the precise determination of it have been pointed out.

Contents

1	Introduction	1
2	Process of preheating	3
2.1	Parametric resonance	3
2.2	End of preheating	4
3	Effect on large scales of CMB	5
4	Calculation of δN	6
4.1	Effect of node shift	8
4.2	Lyapunov Exponent	9
5	δN for particular parameter values	10
5.1	Functional forms of Φ and X	10
5.2	Calculation of X_{\max}	12
5.3	$\frac{g^2}{\lambda} = 2$ case	13
5.4	$\frac{g^2}{\lambda} = 200$ case	15
6	Non-gaussianity	16
7	Conclusion	18
A	Calculation for node shift dependence of $\Delta\mathcal{H}$	19
B	Determination of the necessary quantities	19
C	Expansion of W_y	20

1 Introduction

Preheating is expected to be a mechanism for producing non-gaussian curvature perturbation in super-horizon scales [1–9]. It is agreed in consensus that during preheating highly nonlinear and non-gaussian curvature perturbations generate in small scale [10–12]. But if it is asked that how much effect on the large scales of Cosmic Microwave Background(CMB) can be generated by preheating, the answers vary in a wide range. To predict if the curvature perturbation produced during preheating era can contribute substantially one needs to know the functional form of curvature perturbation in small scales [13]. Here we present a formulation to analytically calculate curvature perturbation from preheating which gives a good match with lattice results[10]. This allows us to establish a connection between the different types of processes during preheating and curvature perturbation produced due to them. Finally we derive the analytical form of effective curvature perturbations on large scales and estimate the amount of non-gaussianity arising from it.

The topic of super-horizon curvature perturbation and local form non-gaussianity produced during preheating has been addressed in many different ways in the literature. Evolution of first order curvature perturbation was observed in [14–17] for the matter fields having solutions of the form of reheating or preheating era. Later the authors of Ref. [1, 2] solved Einstein’s equation with second order curvature

perturbation for the period of preheating, and took the limit $k \rightarrow 0$ of the solution. A high value of non-linearity parameter f_{NL} was reported to be coming from preheating in different models [1, 7]. But there are some restrictions of this formulation, since it is neither a fully nonlinear approach to calculate preheating contribution, nor the gauge invariant combination of perturbations are well defined in second order [18–20]. To avoid this problem very recently covariant formulation has been used in deriving amplification of entropic modes during preheating period [21]. There is another approach which uses “separate universe approximation” or δN formulation [3–6]. In this formalism first curvature perturbation in small scales was calculated using lattice simulation or other methods. After that it was smoothed out with a suitable Gaussian window function and then its effect on CMB was predicted. We follow this second approach in our work.

Separate universe approximation or the δN formulation was first used in the context of preheating in Ref [22, 23]. This formulation tells that the curvature perturbation on super horizon scales can be written in terms of the difference in the number of e -foldings(N) of different causally disconnected patches of the universe on constant density gauge[24, 25]. And the dependence of δN with fields’ perturbation on the super-horizon scales can be written as[26],

$$\zeta(x) = \delta N(x) = \frac{\partial N}{\partial \phi_I} \delta \phi_I(x) + \frac{\partial^2 N}{\partial \phi_I \partial \phi_J} \delta \phi_I(x) \delta \phi_J(x). \quad (1.1)$$

Therefore, if one can calculate the dependence of the N with respect to the background field values ϕ_{Is} , curvature perturbation can be calculated in terms of field perturbations. Keeping this prospect in mind first lattice simulation to calculate δN for different background values of the secondary field(say χ) during preheating was attempted by the authors of Ref.[5, 6]. But the correct dependence was shown in Ref.[10], where the authors found a “periodic” and “spiky” behavior in $\delta N(\chi)$. Even for some values of χ the height of those spikes are so large that the authors moved on to postulate that “the cold spot” of CMB might have come from the dynamics of preheating.

But even after all these efforts in this direction one thing that could not be concluded properly is the amount of non-gaussianity preheating can produce in CMB. So, when Planck released its data [27], all other mechanisms of producing primordial non-gaussianity got constrained, but nothing could be said about preheating. The seed of the uncertainty in this question lies in the functional form of the curvature perturbation. Lattice result gives spiky pattern, but that pattern can be fitted with a large variety of functional forms and someone cannot logically pick a particular one. Different assumption of functional form can give very different result of f_{NL} [13]. Therefore in this paper we attempt to give a functional form of curvature perturbation from the basic dynamic of preheating, so that this uncertainty can be resolved.

The model of our consideration is

$$V = \frac{\lambda}{4} \phi^4 + \frac{g^2}{2} \phi^2 \chi^2, \quad (1.2)$$

since its lattice simulation is already available in literature and for small value of $\frac{g^2}{\lambda}$ it has been predicted to provide detectable non-gaussian signature in CMB[10]. Although $\lambda \phi^4$ potential has been observationally ruled out to be a candidate of inflation potential[28], studying this model for preheating era is still important. It is because some possible potential form for small field inflation can also be approximated as $\lambda \phi^4$ during the oscillation of ϕ around minima[29]. That means the Klein-Gordon equation for χ would have same mathematical form as in the $\lambda \phi^4$ potential.

Difference in the number of e -foldings(δN) in different causally disconnected patch of the universe with different initial background values of χ (say χ_i) gives curvature perturbation. $\delta N(\chi_i)$ is observed at a fixed time sufficiently after the end of preheating. Different values of χ_i drive the Hubble parameter $H(t)$ differently, and difference in $\int H(t)dt$ gives the $\delta N(\chi_i)$. Since δN formulation is defined in constant

density gauge we have to evaluate $\int H(t)dt$ up to the time when that particular patch reaches a fixed value of H . If t_e^0 and t_e are the required time for the disconnected patches with $\chi_i = 0$ and χ_i nonzero, to reach H we have

$$\delta N(\chi_i) = \int_0^{t_e} H(\chi_i, t)dt - \int_0^{t_e^0} H(0, t)dt . \quad (1.3)$$

So, $\delta N(\chi_i)$ can be evaluated if we can calculate how does different $H(t)$ trajectories with different initial conditions move away or towards each other.

We divide this paper in the following sections. In section 2 and 2 we briefly describe the necessary concepts required for the calculations done in the next sections. In section 4 we will describe how can we calculate δN from the bifurcation of the Hubble trajectories. Then in the section 5 we will show that we can assume some particular form of potential and kinetic energy terms and using those we can calculate δN for certain choices of g^2 and λ . Comparison of lattice result and our expression will be shown in that section. In section 6 we smooth out the δN on large scale. This requires a particular value of spatial variance of χ field which corresponds to a certain scale of interest. The smoothed out function gives us the necessary functional form of δN required to calculate f_{NL} . After calculating f_{NL} we move on to the following section 7 where we discuss the findings and the possible outcome of our research. Necessary calculations and used techniques are described in three appendices A, B and C.

2 Process of preheating

Before we begin describing the method for calculating δN , we will very briefly review process of preheating in this section which will be required to develop the discussions in next sections.

2.1 Parametric resonance

After the end of inflation inflaton ϕ oscillates around the minima of the potential and this oscillation pumps up the creation of χ particle. For the potential of Eq. (1.2) equation of motion for the classical background $\phi(t)$ becomes

$$\ddot{\phi} + 3H\dot{\phi} + \lambda\phi^3 = 0 . \quad (2.1)$$

Here dot means derivative w.r.t time(t). This equation gives a solution of $\phi(t)$ which oscillates but its amplitude decays with time. So one moves to use conformal variables $d\eta = \frac{dt}{a}$, $\Phi(\eta) = a\phi(\eta)$ and $X(\eta) = a\chi(\eta)$. This allows one to write Eq. (2.1)

$$\frac{\partial^2 \Phi}{\partial \eta^2} + \lambda\Phi^3 = 0 . \quad (2.2)$$

Unlike the $m^2\phi^2$ potential in this case the Φ does not oscillates sinusoidally, but the solution of this equation can be written as $\Phi(\eta) = \tilde{\Phi}f(x)$, where $x = \sqrt{\lambda}\tilde{\Phi}\eta$, $\tilde{\Phi}$ is the amplitude of oscillation and $f(x)$ is given by Jacobi elliptic function as

$$f(x) = \text{cn} \left(x - x_0, \frac{1}{\sqrt{2}} \right) . \quad (2.3)$$

Elliptic function $f(x)$ can be expressed as a series of cosine functions. The leading order term is $c_0 \cos(0.8472x)$ where $c_0 \approx 1$. Amplitudes of the higher order terms fall off quite fast. The oscillation of classical field ϕ

drives the parametric resonance of the quantum field $X(\eta)$. The mode equation of the k -th mode of $X(x)$ takes the following form

$$X_k'' + \left(\kappa^2 + \frac{g^2}{\lambda} \text{cn}^2 \left(x, \frac{1}{\sqrt{2}} \right) \right) X_k = 0. \quad (2.4)$$

Here derivative has been taken w.r.t. x and $\kappa^2 = \frac{k^2}{\lambda \tilde{\Phi}^2}$. This equation is a type of Lamé equation. The solution of this equation grows as $X_k \propto e^{\mu_k x}$, where μ_k is the characteristic exponent of the corresponding k mode. Value of μ_k depends on the value of $\frac{g^2}{\lambda}$ and k . Maximum value it can attain is 0.2377. From the stability-instability chart of [11, 30] one can figure out that for $\frac{g^2}{\lambda} = 2$, μ_k reaches maximum value for $k = 0$ mode.

Mode equation for Φ becomes

$$\Phi_k'' + \left(\kappa^2 + 3 \text{cn}^2 \left(x, \frac{1}{\sqrt{2}} \right) \right) \Phi_k = 0. \quad (2.5)$$

This equation is nothing but a particular case of Eq. (2.4). Maximum growth of the inhomogeneous modes of Φ_k occurs for $\kappa = 1.6$.

We will use these solutions as inputs in our calculation of δN in section 5.

2.2 End of preheating

Second stage of preheating when the amplification of χ and ϕ field affect the parametric resonance, is known as back-reaction. Thus the frequency of the Φ oscillation increases significantly and the amplitude of the Φ decreases. In the first phase of preheating the the number density of the ϕ particle, say n_k^ϕ increases and the drains away the energy from the Φ field. Increase of $\langle \delta\phi^2 \rangle$ can happen in two ways. First one is parametric resonance described above and second one is rescattering.

Rescattering is the process of production of ϕ particles from the $g^2\phi^2\chi^2$ interaction term. Since the number density of χ particle increases exponentially this process becomes more effective at the last stage of preheating. In fact the parametric amplification of $\langle \delta\phi^2 \rangle$ is much less efficient than the rescattering effect.

Amplitude of $\langle \delta\phi^2 \rangle$ is proportional to the squared of the number density of χ particle (say n_k^χ), where as n_k^χ is proportional to the $\langle \chi^2 \rangle$. This means $\langle \delta\phi^2 \rangle \propto \exp(4\mu x)$. This amplification of $\langle \delta\phi^2 \rangle$ can affect the parametric resonance in two ways. If the leading mode in $\langle \delta\phi^2 \rangle$ have the same frequency and direction of oscillation as the background mode $\Phi(\eta)$, then its effect is indistinguishable from the oscillation of $\Phi(\eta)$. But it would change the amplitude of the oscillation and thus it can change the effective mass of the χ particle, which shifts the parameters of Eq. (2.4) from resonance band to non-resonance band and forces the shut-down of parametric resonance. This process is known as the restructuring of resonance. In modified case $\frac{\tilde{g}^2}{\lambda}$ should look like

$$\frac{\tilde{g}^2}{\lambda} = \frac{g^2}{\lambda} \frac{\Phi^2(\eta) + \langle \delta\phi^2 \rangle}{\tilde{\Phi}^2} = \frac{g^2}{\lambda} \left(1 - 9.2 \frac{\langle \delta\phi^2 \rangle}{\tilde{\Phi}^2} + \frac{\langle \delta\phi^2 \rangle}{\tilde{\Phi}^2} \right) = \frac{g^2}{\lambda} \left(1 - 8.2 \frac{\langle \delta\phi^2 \rangle}{\tilde{\Phi}^2} \right) \quad (2.6)$$

For the derivation of the second step see the relationship between $\Phi(\eta)$ and $\tilde{\Phi}$ in [30]. We can see that for the increase in $\langle \delta\phi^2 \rangle$ in the same direction of $\Phi(\eta)$ oscillation, $\tilde{\kappa}^2$ remains unchanged and $\frac{\tilde{g}^2}{\lambda}$ decreases with time. For $k = 0$ mode from the stability-instability chart of [30] we can see that the $\frac{\tilde{g}^2}{\lambda}$ should have a shift of $\mathcal{O}(1)$ from $\frac{g^2}{\lambda} = 2$ to stop the resonance.

On the other hand if the leading mode of $\langle \delta\phi^2 \rangle$ has much higher frequency than the $\Phi(\eta)$ and comparable amplitude to it, this can go in negative direction in a short time range. So that in a short time span

the oscillating function of the Eq. (2.4) i.e. the $\text{cn}(x, \frac{1}{\sqrt{2}})$ will be modified and the parametric resonance will be stopped.

Among all the effects described above one or more than one of them can be responsible for the end of preheating. It varies from model to model which particular process plays more important role than others. For our model $\lambda\phi^4$ it has been shown[30] that the decrease in $\Phi(\eta)$ and thus the restructuring of resonance is the main cause for the end of preheating. Although calculations in that work did not consider the presence of background χ field value.

3 Effect on large scales of CMB

Modes of the curvature perturbation which crossed horizon during initial period of inflation has much larger wavelength than those modes which leaves horizon during end of inflation. Minimum resolvable wavelength in CMB is around e^{15} times smaller than the largest wavelength. So if inflation ends at 60 e -foldings after the largest wavelength crossed the horizon, wavelengths of interest during preheating is e^{45} times smaller than the minimum resolvable wavelength in CMB. This huge hierarchy of scales ensures that even if a sizable amount of non-gaussian curvature perturbation is produced during preheating its effect on large scales CMB might be washed away. To predict how much imprint this small scale dynamics can leave on CMB the following method was developed[31, 32].

Let's say H_i is the Hubble parameter at the end of inflation. Therefore amplitude of the power spectrum of the χ field's perturbation is $P_\chi = H_i^2$. So, the spatial variance of the χ field can be calculated as[33]

$$\langle \chi(x)^2 \rangle = \int \frac{d^3k}{(2\pi)^3} \frac{P_\chi}{k^3} = \frac{P_\chi}{(2\pi)^2} \ln(q_{\max}L) \quad (3.1)$$

where L is the length of the box size in which perturbation is defined and q_{\max} is the frequency corresponds to H_i . From our above discussion it is evident that for our scales of interest $\ln(q_{\max}L) \approx 45$. We will use this spatial variance as σ of a Gaussian function to be used for smoothing out the curvature perturbation of small scales.

$$\sigma^2(L) = \left(\frac{H_i}{2\pi} \right)^2 45 \quad (3.2)$$

If W is a Gaussian function with this sigma, then smoothed δN , say δN_R , is written as

$$\delta N_R(\chi') = \int_{-\infty}^{\infty} \delta N(\chi) W(\chi' - \chi) d\chi. \quad (3.3)$$

We have two scalar fields in our system, inflaton ϕ and the secondary field χ . So we write down the curvature perturbation on large scales following Eq. (1.1) as

$$\zeta(x) = N_\phi^{\text{inf}} \delta\phi(x) + N_\phi^{\text{pre}} \delta\phi(x) + N_\chi^{\text{pre}} \delta\chi(x) + \frac{1}{2} N_{\chi\chi}^{\text{pre}} \delta\chi^2(x). \quad (3.4)$$

Here two things are assumed, firstly the contribution of χ field during inflation is negligible and secondly inflaton ϕ does not produce any second order curvature perturbation during preheating. If we go to the Fourier space we get

$$\zeta_k = \underbrace{N_\phi^{\text{inf}} \delta\phi_k + N_\phi^{\text{pre}} \delta\phi_k}_{\zeta_k^\phi} + \underbrace{N_\chi^{\text{pre}} \delta\chi_k + \frac{1}{2} N_{\chi\chi}^{\text{pre}} \int \frac{d^3p}{(2\pi)^3} \delta\chi_p \delta\chi_{k-p}}_{\zeta_k^\chi}. \quad (3.5)$$

We take one more assumption that is the contribution from perturbation of ϕ and χ are uncorrelated i.e. $\langle \zeta_k^\phi \zeta_k^\chi \rangle = 0$ which allows us to write the 2-point correlation as

$$\begin{aligned} \langle \zeta_{k_1} \zeta_{k_2} \rangle &= \langle \zeta_{k_1}^\phi \zeta_{k_2}^\phi \rangle + \langle \zeta_{k_1}^\chi \zeta_{k_2}^\chi \rangle \\ &= N_\phi^2 \langle \delta\phi_{k_1} \delta\phi_{k_2} \rangle + (N_\chi^{\text{pre}})^2 \langle \delta\chi_{k_1} \delta\chi_{k_2} \rangle + \\ &\quad \frac{1}{4} (N_{\chi\chi}^{\text{pre}})^2 \int \frac{d^3 p_1 d^3 p_2}{(2\pi)^6} \langle \delta\chi_{p_1} \delta\chi_{k_1-p_1} \delta\chi_{p_2} \delta\chi_{k_2-p_2} \rangle \end{aligned} \quad (3.6)$$

and the 3-point correlation as

$$\begin{aligned} \langle \zeta_{k_1} \zeta_{k_2} \zeta_{k_3} \rangle &= \frac{1}{2} (N_\chi^{\text{pre}})^2 N_{\chi\chi}^{\text{pre}} \int \frac{d^3 p_1}{(2\pi)^3} \{ \langle \delta\chi_{p_1} \delta\chi_{k_1-p_1} \delta\chi_{k_2} \delta\chi_{k_3} \rangle + \text{permutations} \} + \\ &\quad \frac{1}{8} (N_{\chi\chi}^{\text{pre}})^3 \int \frac{d^3 p_1 d^3 p_2 d^3 p_3}{(2\pi)^9} \langle \delta\chi_{p_1} \delta\chi_{k_1-p_1} \delta\chi_{p_2} \delta\chi_{k_2-p_2} \delta\chi_{p_3} \delta\chi_{k_3-p_3} \rangle \end{aligned} \quad (3.7)$$

Defining F_{NL} as the ratio of bi-spectrum to the squared of power spectrum [34–36] we get

$$\begin{aligned} F_{\text{NL}}^{\text{local}} &= \frac{5}{3} \frac{\langle \zeta_{k_1} \zeta_{k_2} \zeta_{k_3} \rangle}{\langle \zeta_{k_1} \zeta_{k_2} \rangle^2 + \text{permutations}} \Big|_{k_1=k_2=k \gg k_3} \\ &= \frac{5}{6} (N_\chi^{\text{pre}})^2 N_{\chi\chi}^{\text{pre}} \frac{P_\chi^2}{P_\zeta^2} + \frac{5}{48} (N_{\chi\chi}^{\text{pre}})^3 \frac{P_\chi^3}{P_\zeta^2} \end{aligned} \quad (3.8)$$

In general local form non-gaussianity is defined to be the case where ζ can be written as $\zeta_g + \frac{3}{5} f_{\text{NL}} \zeta_g^2$. This is not possible in case of our interest. But exactly like the standard local form non-gaussianity, this kind of non-gaussianity is also expected to show up in the squeezed limit of the bispectrum.

From the discussions presented at the beginning of this subsection we can say that here δN_R will play the role of δN^{pre} . So we can understand that depending on the form of δN_R either the first term or the second term in Eq. (3.8) will play important role in the value of f_{NL} . But all these discussions are based upon one assumption that is expansion of δN_R can be terminated upto certain order. If it is not true then the situation become more complex[13].

4 Calculation of δN

In the evolution of $H(t)$ three energy terms contribute, viz, potential energy, kinetic energy and gradient energy. But upto the last stage of preheating we can neglect the contribution from gradient energy. This assumption enables us to cast the Friedmann equation into the following form,

$$\dot{H}(t) + 3H^2(t) \approx 8\pi V(t) \ , \quad (4.1)$$

where dot means derivative with respect to t . In the above equation amplitude of $V(t)$ drops gradually with time. But if we change the variables as, $d\tau = dt/a(t)^2$, $\mathcal{H} = a^2 H$, $\Phi = a\phi$ and $X = a\chi$, the amplitude of $\mathcal{V}(\tau)$ remains almost constant with τ . Hence Eq. (4.1) is rewritten as,

$$\frac{d\mathcal{H}(\tau)}{d\tau} + \mathcal{H}^2(\tau) \approx 8\pi \mathcal{V}(\tau) \ , \quad (4.2)$$

where \mathcal{V} becomes

$$\mathcal{V} = \frac{\lambda}{4} \Phi^4 + \frac{g^2}{2} \Phi^2 X^2. \quad (4.3)$$

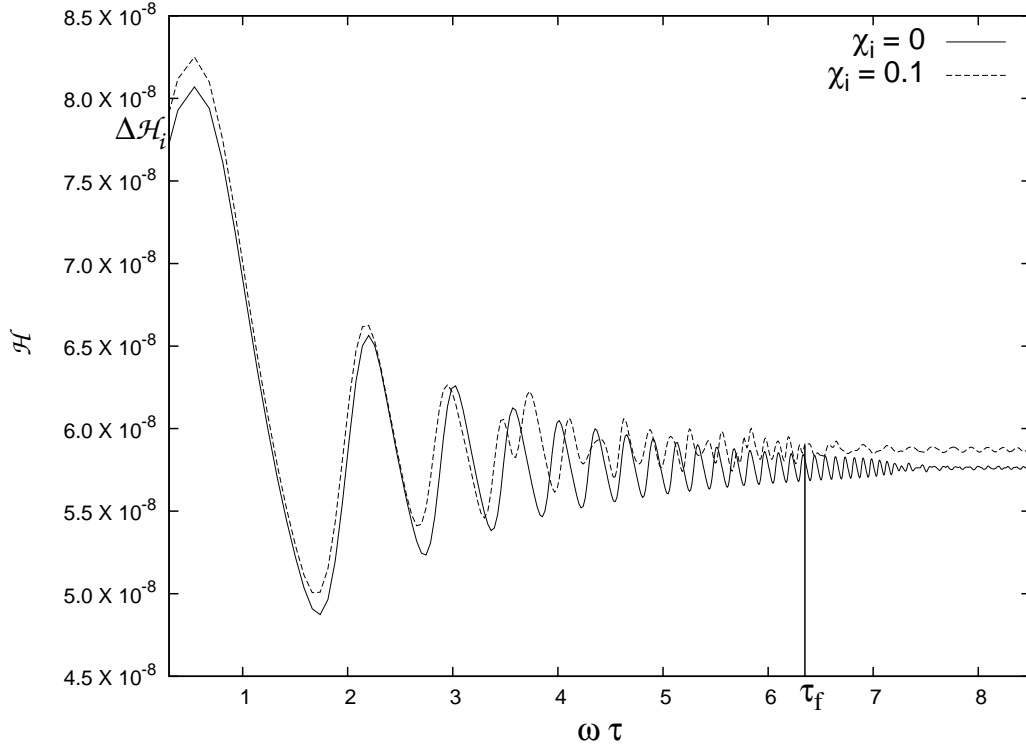


Figure 1. \mathcal{H} trajectories oscillates with τ and unlike cases with fixed singular points different trajectories with different initial \mathcal{H} values cross each other. τ_f is the time when the oscillation in the in \mathcal{H} trajectory freezes, which means that preheating process has been finished. Naturally τ_f varies for different trajectories. This plot is generated with lattice simulation for $\frac{q^2}{\lambda} = 2$. A very high value of $\chi_i = 0.1$ has been taken to magnify the difference in the \mathcal{H} trajectories to a visible level.

During the period of preheating process, \mathcal{V} is an oscillatory function. In the evolution of \mathcal{H} , we would have seen standard saddle-node bifurcation feature from this equation if \mathcal{V} was constant with τ . That means in the one-dimensional space of \mathcal{H} , there would have been a saddle point from which \mathcal{H} would have move away while τ increases. There should be another stationary point in this one-dimensional space which attracts the trajectories towards it. That point is termed as node. We have checked that this saddle-node feature in \mathcal{H} trajectories remains even if \mathcal{V} oscillates with constant amplitude (see Fig. 1). Since initial values of \mathcal{H} are always positive, all the $\mathcal{H}(\tau)$ trajectories move towards node and away from saddle.

Now we divide the total time span of the integration of Eq. (1.3) in two different parts. First part is the period of exponential growth of the X field which starts from $\tau = 0$ and grows upto $\tau = \tau_f$. Second period starts at $\tau = \tau_f$ and continues upto $\tau = \tau_e$. The latter period behaves mostly like radiation dominated era. So, the Eq. (1.3) can be re-casted into

$$\delta N(\chi_i) = \int_0^{\tau_f} (\mathcal{H}(\chi_i, \tau) - \mathcal{H}(0, \tau)) d\tau + \int_{\tau_f}^{\tau_e} \mathcal{H}(\chi_i, \tau) d\tau - \int_{\tau_f}^{\tau_e^0} \mathcal{H}(0, \tau) d\tau . \quad (4.4)$$

Here superscript “0” indicates the value of these time limits for $\chi_i = 0$ trajectory. Both the trajectories reach at Hubble value H_e at τ_e and τ_e^0 respectively.

In this latter period, i.e., from τ_f to τ_e , we assume the scale factor a changes with physical time t as $a(t) = \left(a_f^{1/\alpha} + ct - ct_f \right)^\alpha$. If w is the equation of state parameter then $\alpha = \frac{2}{3(1+w)}$ and c is a constant

whose value is given by initial energy density. This gives

$$\int_{\tau_f}^{\tau_e} \mathcal{H} d\tau = \int_{t_f}^{t_e} H dt = \int_{\mathcal{H}_f/a_f^2}^{H_e} \frac{H}{\dot{H}} dH = -\alpha \log H_e + \alpha \log \mathcal{H}_f - 2\alpha \log a_f . \quad (4.5)$$

Putting this back in Eq. (4.4) we get

$$\delta N(\chi_i) = \int_0^{\tau_f} \Delta \mathcal{H}(\chi_i, \tau) d\tau + \alpha \log \frac{\mathcal{H}_f(\chi_i)}{\mathcal{H}(0, \tau_f)} - 2\alpha \log \frac{a_f}{a^0(\tau_f)} , \quad (4.6)$$

where $\Delta \mathcal{H}(\chi_i, \tau) = \mathcal{H}(\chi_i, \tau) - \mathcal{H}(0, \tau)$.

As expected H_e cancels out and $\delta N(\chi_i)$ remains independent of it. Generally w is expected to be $\frac{1}{3}$ for radiation dominated era but lattice simulation shows it is slightly less than that [37]. Therefore following that for our future purpose we will choose $w = 0.28$, i.e., $\alpha = 0.52$.

Separation between \mathcal{H} trajectories tends to decrease or increase with τ . This rate of decrease or increase in this difference is characterized by the Lyapunov exponent (Λ) simply as,

$$\Delta \mathcal{H}(\tau) = \Delta \mathcal{H}_i e^{\Lambda \tau} , \quad (4.7)$$

where $\Delta \mathcal{H}(\tau)$ is the separation between the trajectories at a particular τ , and $\Delta \mathcal{H}_i$ is the initial difference between two \mathcal{H} 's. These difference is introduced by their initial field values.

4.1 Effect of node shift

Separation of trajectories in Eq. (4.7) would have been sufficient in the calculation of Eq. (4.6) if the amplitude of \mathcal{V} was constant with τ as well as with $\Delta \mathcal{H}_i$. But in reality, for different χ_i , i.e., for different $\Delta \mathcal{H}_i$ preheating ends at different values of τ . The end values of \mathcal{H} are also different as shown in Fig. 1. So, the node point changes with initial conditions. Therefore the stationary points are movable. There is no definite prescription in the literature to answer how this change in node value modifies Eq. (4.7). Here we take a quasi-static approach to see its effect. Node value in the Eq. (4.7) is $\sqrt{8\pi\mathcal{V}}$ (say A). Amplitude and frequency of \mathcal{V} vary with χ_i . So change in A at a particular τ can be written as

$$\Delta A = \frac{\partial A}{\partial \chi_i} \delta \chi_i + \frac{\partial A}{\partial \omega} \frac{\partial \omega}{\partial \chi} \delta \chi_i , \quad (4.8)$$

where ω is the frequency of oscillation of \mathcal{V} .

Solution of Eq. (4.7) with constant \mathcal{V} is

$$\mathcal{H}(\tau) = A \left(\tanh \left(\tau A + \tanh^{-1} \frac{\mathcal{H}_i}{A} \right) \right) . \quad (4.9)$$

If A doesn't change with $\Delta \mathcal{H}_i$ it can be shown that,

$$\Delta \mathcal{H}(\tau) = \Delta \mathcal{H}_i [B(\mathcal{H}_i, A, \tau) A] , \quad (4.10)$$

where $B(\mathcal{H}_i, A, \tau)$ is a function of \mathcal{H}_i , A and τ , whose exact expression is shown in Appendix-A. To calculate Lyapunov exponent for constant \mathcal{V} case we write Eq. (4.2) in the form of difference equation as,

$$\mathcal{H}_{n+1} = \underbrace{\mathcal{H}_n - \mathcal{H}_n^2 + A^2}_{f_n} . \quad (4.11)$$

Definition of Lyapunov exponent is [38, 39]

$$\Lambda = \frac{1}{n} \sum_i^n \log \left| \frac{\partial f_i}{\partial \mathcal{H}} \right| \approx \frac{1}{\tau} \int_0^\tau \log \left| \frac{\partial f}{\partial \mathcal{H}} \right| d\tau' . \quad (4.12)$$

If $A \ll 1$, which is true in our case, $\log[B(\mathcal{H}_i, A, \tau)A]$ matches quite well with the standard definition of Lyapunov exponent multiplied by τ . So we can write

$$B(\mathcal{H}_i, A, \tau)A \approx e^{\Lambda\tau} \quad (4.13)$$

We assume the form of solution of Eq. (4.9) can describe the behaviour of \mathcal{H} when \mathcal{V} changes with time. This is where the quasi-static approximation comes into play. With this assumption we write the difference in the \mathcal{H} trajectories as,

$$\begin{aligned} \Delta\mathcal{H}(\tau) &= \mathcal{H}(\tau, \tilde{A}, \mathcal{H}_i + \Delta\mathcal{H}_i) - \mathcal{H}(\tau, A, \mathcal{H}_i) \\ &= \frac{\mathcal{H}(\tau, \tilde{A}, \mathcal{H}_i + \Delta\mathcal{H}_i) - \mathcal{H}(\tau, A, \mathcal{H}_i)}{B(\mathcal{H}_i, A, \tau)A} e^{\Lambda\tau} \\ &= (\Delta\mathcal{H}_i + C(\mathcal{H}_i, A, \tau)\Delta A) e^{\Lambda\tau} , \end{aligned} \quad (4.14)$$

where $\tilde{A} = A + \Delta A$ and C is a function whose value is of $\mathcal{O}(1)$ (see Appendix A). We will plug in this form of $\Delta\mathcal{H}(\tau)$ in Eq. (4.6) to calculate the value of $\delta N(\chi_i)$.

4.2 Lyapunov Exponent

So far we have dealt with constant A . Now we will vary \mathcal{V} for calculation of Λ . So the difference equations Eq. (4.11) reads as,

$$\mathcal{H}_{n+1} = \underbrace{\mathcal{H}_n - \mathcal{H}_n^2 + 8\pi\mathcal{V}_n}_{f_n} . \quad (4.15)$$

So, using the definition in Eq. (4.12) we write

$$\begin{aligned} \int e^{\Lambda\tau} d\tau &= \int \exp \left\{ \left(\frac{1}{\tau} \int_0^\tau \log \left| \frac{\partial f(\tau')}{\partial \mathcal{H}} \right| d\tau' \right) \tau \right\} d\tau = \int \exp \left\{ \int_0^\tau \left(\log \left| \frac{\partial f(\tau')}{\partial \mathcal{H}} \right| - \mathcal{H} \right) d\tau' \right\} d\eta \\ &= \int \exp \left\{ \int_0^\tau \left(-4\pi \frac{\partial \mathcal{K}}{\partial \mathcal{H}} + 4\pi \frac{\partial \mathcal{V}}{\partial \mathcal{H}} + \dots \right) d\tau' \right\} d\eta \\ &= \int \left(1 + \int_0^\tau \left(1 - 4\pi \frac{\partial \mathcal{K}}{\partial \mathcal{H}} + 4\pi \frac{\partial \mathcal{V}}{\partial \mathcal{H}} \right) d\tau' + \dots \right) d\eta , \end{aligned} \quad (4.16)$$

where $d\eta = \frac{dt}{a(t)}$ and $\mathcal{K} = a^4 K$, with K being the kinetic energy. In the last step we have taken $\frac{\partial \mathcal{K}}{\partial \mathcal{H}}$ and $\frac{\partial \mathcal{V}}{\partial \mathcal{H}}$ to be small compared to one. We have also used Eq. (4.2) and $\mathcal{H}^2 = \frac{8\pi}{3}(\mathcal{V} + \mathcal{K})$ relation. Now we go to a different set of variables \mathcal{P} and \mathcal{E} to perform this integration.

$$\begin{aligned} \mathcal{E} &= \mathcal{V} + \mathcal{K} , \\ \mathcal{P} &= \mathcal{V} - \mathcal{K} . \end{aligned} \quad (4.17)$$

In these variables the continuity equation reads as

$$\frac{\partial \mathcal{E}}{\partial \tau} + 3\mathcal{H}\mathcal{P} - \mathcal{H}\mathcal{E} = 0 . \quad (4.18)$$

Using these we write

$$\int_0^\tau \left(-4\pi \frac{\partial \mathcal{K}}{\partial \mathcal{H}} + 4\pi \frac{\partial \mathcal{V}}{\partial \mathcal{H}} \right) d\tau' = \int_0^\tau 4\pi \frac{3}{4\pi(\mathcal{E} - 3\mathcal{P})} \frac{d\mathcal{P}}{d\tau'} d\tau' = -\log |\mathcal{E}_0 - 3\mathcal{P}| + \log |\mathcal{E}_0 - 3\mathcal{P}_0|. \quad (4.19)$$

In last step we assumed that \mathcal{E} does not change too much with respect to the change in \mathcal{P} . Here \mathcal{E}_0 is the initial value of \mathcal{E} . The quantity $(\mathcal{E}_0 - 3\mathcal{P})$ has a maximum amplitude of $4\mathcal{E}_0$ and \mathcal{P}_0 is equal to \mathcal{E}_0 . Therefore expanding the above result upto second order in \mathcal{P} we get,

$$\begin{aligned} \frac{1}{2} \left(1 - \frac{(\mathcal{E}_0 - 3\mathcal{P})^2}{16\mathcal{E}_0^2} \right) + \dots - \log 2 &= \frac{15}{32} + \frac{3\mathcal{P}}{16\mathcal{E}_0} - \frac{9\mathcal{P}^2}{32\mathcal{E}_0^2} + \dots - \log 2 \\ &= \frac{15}{32} - \frac{3\mathcal{K}}{16\mathcal{E}_0} + \frac{3\mathcal{V}}{16\mathcal{E}_0} - \frac{9\mathcal{K}^2}{32\mathcal{E}_0^2} + \frac{9\mathcal{K}\mathcal{V}}{16\mathcal{E}_0^2} - \frac{9\mathcal{V}^2}{32\mathcal{E}_0^2} + \dots - \log 2. \end{aligned} \quad (4.20)$$

So in-total we write

$$\int e^{\Lambda\tau} d\tau = \int \left(1 + \frac{15}{32} - \frac{3\mathcal{K}}{16\mathcal{E}_0} + \frac{3\mathcal{V}}{16\mathcal{E}_0} - \frac{9\mathcal{K}^2}{32\mathcal{E}_0^2} + \frac{9\mathcal{K}\mathcal{V}}{16\mathcal{E}_0^2} - \frac{9\mathcal{V}^2}{32\mathcal{E}_0^2} + \dots - \log 2 \right) d\eta. \quad (4.21)$$

Here \mathcal{K} can be taken as $\frac{1}{2}\Phi'^2 + \frac{1}{2}X'^2$ for prolonged period of inflaton oscillations.

For the calculation of third term in Eq. (4.6) we need to know the value of a_f from where we can take the assumption of nearly radiation domination as \mathcal{H} as well as a have oscillatory features, we can take the value of a_f to be averaged value of a at τ_f . So we write,

$$-2\alpha \log \frac{a_f}{a^0(\tau_f)} = -2\alpha \int_0^{\tau_f} \Delta \mathcal{H}_{\text{avg}} e^{\Lambda\tau} \Big|_{\text{avg}}. \quad (4.22)$$

As discussed earlier \mathcal{V} is an oscillating even function of τ . So, the second part of Eq. (4.8) is an odd function of τ and the first part is even. Therefore in the integration of the first part of Eq. (4.6) we can expect, for the large values of τ , the effect of the odd part of ΔA will be washed away. So, keeping only the even part and using integration by parts we write

$$\int_0^{\tau_f} \Delta \mathcal{H}(\chi_i, \tau) d\tau \approx \left[\left(\Delta \mathcal{H}_i + C \frac{\partial A}{\partial \chi_i} \delta \chi_i \right) \int e^{\Lambda\tau} d\tau \right]_0^{\tau_f}. \quad (4.23)$$

5 δN for particular parameter values

Here in this section we will first assume some simple form Φ and X motivated by their field dynamics. Then we will use them in \mathcal{K} and \mathcal{V} so that we can perform the integration of Eq. (4.21). Next we will calculate the maximum value achievable by X for zero as well as non-zero χ_i cases. Using this we will calculate ΔH_f and ΔH_i and we will plug them into Eq. (4.23). These calculations will enable us to compute δN_{χ_i} using Eq. (4.6).

5.1 Functional forms of Φ and X

The equations of motion for Φ and X and their solutions have been described in section 2. Elliptic function $\text{cn}(x)$ can be expanded in a series of cosine functions. We will only consider the first term for our calculation, which is proportional to $\cos(0.8472x)$. The solution of the k -th mode of X takes the form $X_k = P(x) \exp(\mu_k x)$ where $P(x)$ is a periodic function in x . Since we have already approximated $\text{cn}(x)$ with $\cos(0.8472x)$ we can write down the Lamé equation of X in Mathieu equation form. From there we

find that $P(x)$ can be approximated as $\cos(nx)$, where n can be any real number. This n gets different values for different $\frac{g^2}{\lambda}$. So we write,

$$\begin{aligned}\Phi(\eta) &= \tilde{\Phi} \cos(\omega\eta) , \\ X(\eta) &= X_i \cos(n\omega\eta) e^{\mu\omega\eta} ,\end{aligned}\tag{5.1}$$

where $\tilde{\Phi}$ is the initial value of Φ field and X_i is the initial background value of X field. If for certain $\frac{g^2}{\lambda}$, background mode of X field doesn't get amplified, then this form of $X(\eta)$ might not hold. But in the cases where it does get amplified, growth of the background mode overshadows the other non-leading modes. In Eq. (5.1) $\omega = 0.8472\sqrt{\lambda}\tilde{\Phi}$ and μ is the maximum of the characteristic exponents $\mu(k)$. Integration limit η_f is the time when X reaches its maximum amplitude X_{\max} . This gives us

$$\eta_f = \frac{\log \frac{X_{\max}}{X_i}}{\mu\omega} .\tag{5.2}$$

Using these assumptions now we write

$$\mathcal{V} = \frac{1}{4}\lambda\Phi^4 \cos^4(\omega\eta) + \frac{1}{2}g^2\chi_i^2 e^{2\mu\omega\eta}\Phi^2 \cos^2(\omega\eta) \cos^2(n\omega\eta) ,\tag{5.3}$$

and

$$\begin{aligned}\mathcal{K} &= \frac{1}{2}\omega^2\Phi^2 \sin^2(\omega\eta) + \frac{1}{2}e^{2\eta\mu\omega}\omega^2\mu^2\chi_i^2 \cos(n\omega\eta)^2 \\ &\quad - e^{2\eta\mu\omega}\omega^2n\mu\chi_i^2 \cos(n\eta\omega) \sin(n\eta\omega) + \frac{1}{2}e^{2\eta\mu\omega}n^2\omega^2\chi_i^2 \sin(n\omega\eta)^2 .\end{aligned}\tag{5.4}$$

We have deliberately written $X_i = \chi_i$ because $a = 1$ at initial time and the form of Eq. (5.1) is suitable for the cases where background mode gets the maximum amplification. Now we can plug in these forms in Eq. (4.21) and do the integrations.

For the calculation of Eq. (4.23) we need the initial value of $\Delta\mathcal{H}$ and the node shift value $\frac{\partial A}{\partial\chi}\delta\chi$ at initial and final times. Calculation of the initial value is straightforward and can be written as,

$$\Delta\mathcal{H}_i = \sqrt{\frac{8\pi}{3}\lambda\left(\frac{1}{4}\tilde{\Phi}^4 + \frac{g^2}{2\lambda}\chi_i^2\tilde{\Phi}^2\right)} - \sqrt{\frac{8\pi}{3}\lambda\frac{\tilde{\Phi}^4}{4}} .\tag{5.5}$$

The difference in the node values at the end of preheating between two trajectories with χ_i equals to zero and χ_i non-zero (say, $\Delta\mathcal{H}_f$) is

$$\begin{aligned}\frac{\partial A}{\partial\chi}\delta\chi = \Delta\mathcal{H}_f &= \sqrt{8\pi\lambda\left(\frac{1}{4}\Phi^4(\eta_f) \cos^4(\omega_\Phi\eta_f) + \frac{g^2}{2\lambda}X_{\max}^2\Phi^2(\eta_f) \cos^2(\omega_\Phi\eta_f) \cos^2(n\omega\eta_f)\right)} \\ &\quad - \sqrt{8\pi\lambda\left(\frac{1}{4}\Phi^4(\eta_f) \cos^4(\omega_\Phi\eta_f) + \frac{g^2}{2\lambda}X_{\text{sat}}^2\Phi^2(\eta_f) \cos^2(\omega_\Phi\eta_f) \cos^2(n\omega\eta_f)\right)} .\end{aligned}\tag{5.6}$$

Here X_{sat} is the value of the field for which X reaches its maximum amplitude in zero χ_i case and ω_Φ is the frequency of oscillation of Φ at the last stage of preheating.

In performing the integration of Eq. (4.21) we will not consider the change in the frequency of Φ oscillation with time. This is because the change in ω mostly happens at the final stage of preheating and contribution of that small range of τ is negligible in integration of Eq. (4.21).

5.2 Calculation of X_{\max}

The field $X(\eta)$ can be thought of an exponentially growing function up to η_f . But precisely speaking this co-moving time does not actually signify the end of resonance of the background mode of X [40]. Rather background mode reaches the saturation value (X_{sat}) little earlier than η_f . And after the saturation of the background mode, the inhomogeneous modes continue to grow for a little while. In this section we will attempt to calculate X_{\max} which is the maximum amplitude of X from some arguments of energy conservation and will see how it varies with initial background values of χ .

We have seen in Section 2 that the main effect which terminates the resonance of the background mode of X_k , is the restructuring of the resonance band. Let ξ be the value of $\frac{q^2}{\lambda}$ for which resonance terminates. Therefore we see from Eq. (2.6) that $\langle \delta\Phi^2 \rangle$ has to increase up to the following value,

$$\langle \delta\Phi^2 \rangle = \left(1 - \frac{\lambda\xi}{g^2}\right) \frac{\tilde{\Phi}^2}{8.2} \quad (5.7)$$

For the problem in our hand we have to figure out how this $\langle \delta\Phi^2 \rangle$ changes with the initial background field values of χ . Production of χ particle from the background classical field ϕ has been described as the scattering of χ particles with the homogeneous condensate of ϕ particles [41, 42]. But here the opposite thing needs to be studied, i.e., the scattering of ϕ particle with the homogeneous condensate of χ particle. Addressing this problem is out of the scope of this paper.

Therefore we give some logical arguments following the line of [40] to get the dependence of $\langle X^2 \rangle$ with χ_i and thus the relation between X_{\max} and χ_i . First we will look at the $\chi_i = 0$ case. We assume that $\langle \delta\Phi^2 \rangle$ is proportional to X^2 . It is expected if the production of $\langle \delta\Phi^2 \rangle$ is mainly due to the rescattering, not the parametric resonance. If $\langle \delta\Phi^2 \rangle = \sigma X^2$ then we can write the saturation value of X^2 as

$$X_{\text{sat}}^2 = \left(1 - \frac{\lambda\xi}{g^2}\right) \frac{\tilde{\Phi}^2}{10.3\sigma}. \quad (5.8)$$

For example in $\frac{q^2}{\lambda} = 2$ case, the lattice result gives us the value of $X_{\text{sat}}^2 = 0.39$ (see Fig. 4). From the discussions in subsection 2.2 it is evident that $\xi = 1$. Hence we can determine the value of σ to be 0.05. Now we move on to calculate the relation between the kinetic energies of these fields. Since $\langle \delta\phi^2 \rangle$ gets its kinetic energy from the kinetic energy of X particle we can write

$$\frac{\kappa_{\Phi}^2}{2} \langle \delta\Phi^2 \rangle = \theta \frac{\kappa_X^2}{2} \langle \delta X^2 \rangle. \quad (5.9)$$

Here κ_{Φ} and κ_X is the leading mode in $\langle \delta\Phi^2 \rangle$ and $\langle \delta X^2 \rangle$ respectively and θ is the fraction which determines the amount of kinetic energy transferred to ϕ particle. We know that the Lamé equation Eq. (2.4) and Eq. (2.5) for X_k and Φ_k respectively are just the same equation with different $\frac{q^2}{\lambda}$ parameters. So from the stability-instability chart of [30] we can figure out that κ_X is much lower than the κ_{Φ} . We find $\frac{\kappa_{\Phi}^2}{\kappa_X^2}$ is close to 16. Using the value of σ we determine the value of $\theta = 0.8$. So the way we have calculated θ for $\frac{q^2}{\lambda} = 2$ case, we can determine its value for other $\frac{q^2}{\lambda}$ cases.

Now we introduce nonzero value of χ_i . One can think of it as the homogeneous condensate of particle and its kinetic energy will contribute to the available kinetic energy for the production of Φ particles. So we expect that the amplitude of $\langle \delta\Phi^2 \rangle$ increases due to it. We have checked with lattice simulation [43] that number density of Φ particles increases substantially with the introduction of χ_i . That means although the parametric resonance of the background mode and the low momentum modes of X end earlier than that

of the zero χ_i case, the extra growth of $\langle \delta\Phi^2 \rangle$ will decay into X particle and produce some more $\langle \delta X^2 \rangle$. We write X_{\max}^2 as the combination of X_{sat}^2 and this extra $\langle \delta X^2 \rangle$.

For the given potential of Eq. (4.3), the scattering cross-section from Φ to X in vacuum is [40]

$$\sigma_{\text{scatt}} \approx \frac{g^2}{16\pi\tilde{\Phi}^2}. \quad (5.10)$$

But the actual rate of scattering will be multiplied by the number density of the Φ particle (n_{κ}^{Φ}) since there is a huge number of Φ and X particles in the medium. Extra kinetic energy due to nonzero χ_i is of the order of $\frac{\mu^2\omega^2\chi_i^2}{4}e^{2\mu\omega\eta_f^0}$ with η_f^0 is the comoving time when X reaches its saturation value X_{sat} for $\chi_i = 0$ case. So the extra $\langle \delta\Phi^2 \rangle$ can be determined using Eq. (5.9). Extra $\langle \delta X^2 \rangle$ will be $\sigma_{\text{scatt}}n_{\Phi}$ times the extra $\langle \delta\Phi^2 \rangle$. Therefore we can write

$$X_{\max}^2 = X_{\text{sat}}^2 + \beta\chi_i^2, \quad (5.11)$$

where $\beta = \theta\sigma_{\text{scatt}}n_{\Phi}\frac{\mu^2}{\kappa_{\Phi}^2}e^{2\mu\omega\eta_f^0}$. The above expression is an approximate expression and derived without detailed calculation of scattering between Φ particle and homogeneous condensate of X particles. Any detailed calculation in this direction might modify Eq. (5.11) and thus the shape of $\delta N(\chi_i)$.

Determination of X_{sat} and η_f^0 has been done using lattice simulation. It could have been calculated analytically by considering back-reaction under some approximate analytical method like Hartree approximation, as it has been taken in [15, 17]. But in that case there was a possibility of overestimating these quantities, i.e. underestimating the effect of back-reaction. In [16] η_f^0 has been calculated to be around $\frac{80}{\sqrt{\lambda\Phi}}$ for $\frac{g^2}{\lambda} = 2$. But lattice simulation(see Fig. B) indicates it to be $\frac{59}{\sqrt{\lambda\Phi}}$. Since X is an exponentially growing function such over estimate would lead to a high value of δN , as expected in [15, 16, 21]. But lattice result of δN [10] shows us that in small χ_i region values of δN are well within the observed limit.

5.3 $\frac{g^2}{\lambda} = 2$ case

Dynamics of preheating varies drastically for different values of $\frac{g^2}{\lambda}$ parameter. For $\frac{g^2}{\lambda} = 2$ case it is the $\kappa = 0$ mode which gets maximum amplification. Using the assumed form of $X(\eta)$, $\Phi(\eta)$ and other necessary quantities as described in subsection 5.1 and 5.2 we evaluate Eq. (4.21). For this choice of $\frac{g^2}{\lambda}$, X_{sat} gets a value of 0.39 and n becomes 1. ω_{Φ} comes out to be $\sim 3.3\omega$. Since at the end of preheating when resonance stops we expect the frequency of X remain equal to the driving frequency 3.3ω . This gives us the high frequency of $\Delta\mathcal{H}_f$. The ascending slope of $\Delta\mathcal{H}_f$ and thus $\delta N(\chi_i)$ comes from the relation between X_{\max} and X_{sat} , Eq. (5.11). In the expression of β of Eq. (5.11) value of n_{Φ} has been taken to be as high as 10^9 following the result of lattice simulation using [43] for non zero χ_i . η_f^0 comes to be $\frac{59}{\sqrt{\lambda\Phi}}$ (see Appendix B).

The first term in Eq. (4.6) is calculated using Eq. (4.23). In the combination $\Delta\mathcal{H}_i + C\Delta\mathcal{H}_f$, contribution of $\Delta\mathcal{H}_i$ is negligible compared to the latter term. Variation of $\Delta\mathcal{H}_f$ has been shown in first panel of Fig. 2.

Different quantities calculated in this process are shown in Fig. 2. $\int_0^{\tau_f^0} \mathcal{H}(0, \tau)d\tau$ does not impart significant contribution in the δN and integration of Lyapunov exponent is also not sensitive to the last stage of the preheating. $\Delta\mathcal{H}_i$ is always negligible compared to $\Delta\mathcal{H}_f$. There for only these three terms shown in this figure contribute. We do not show the total expression for $\delta N(\chi_i)$ to avoid complexity. But approximate expression will be shown later.

One can see the plot contains all the features shown in the lattice result in [10]. But the dependence of X_{\max} with χ_i is an issue needs to be addressed in much details. How can χ_i influence the increase in total χ particle production even after the end of parametric resonance has to be addressed to get the right slope

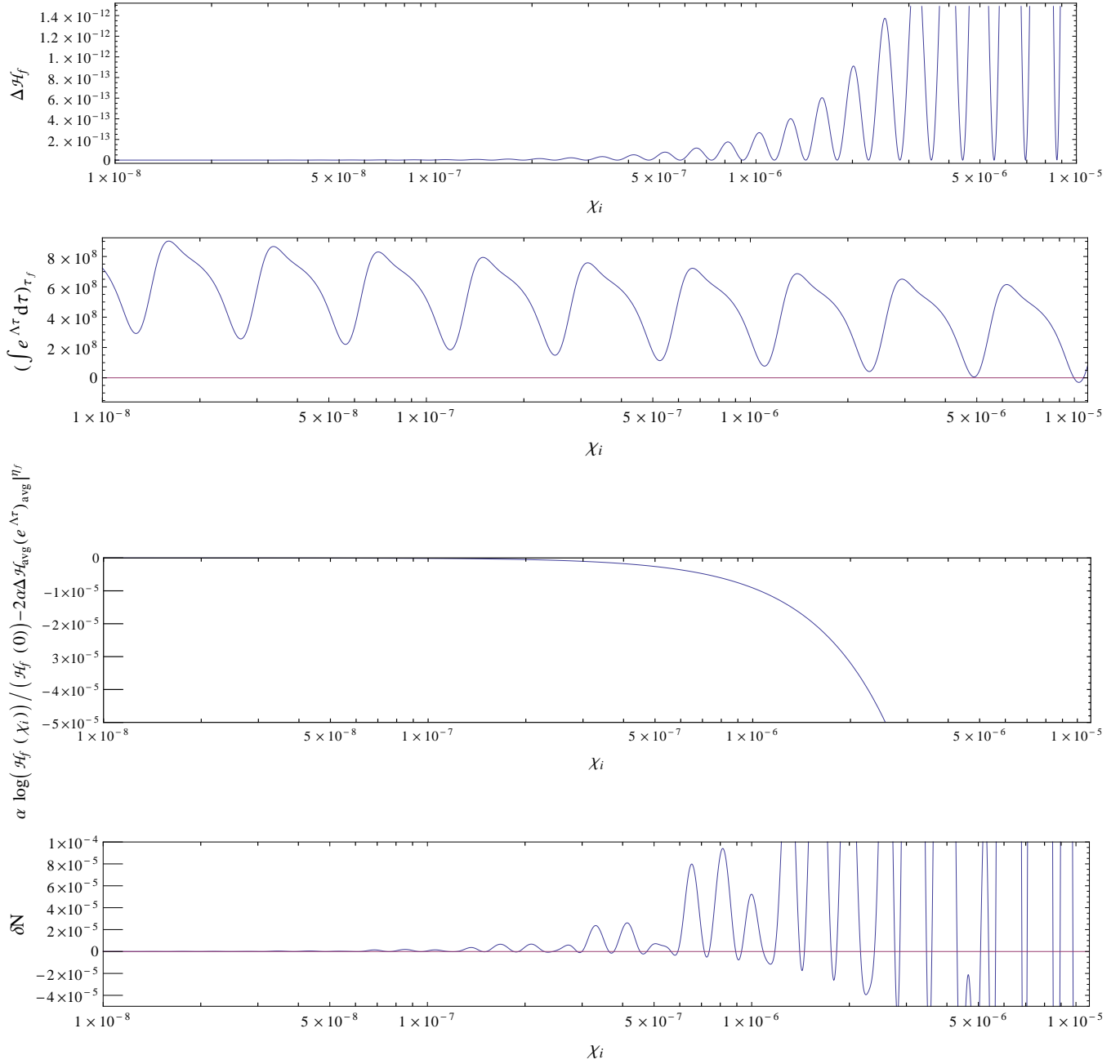


Figure 2. This plot is drawn from Eq. (4.6) with $\frac{q^2}{\lambda}=2$ and $\lambda = 1 \times 10^{-13}$. Since all other terms do not make substantial contribution these three quantities of the three upper panels make up the δN . First and second quantities get multiplied and adds up to the third one to produce total δN in lowest panel. Lattice result for $\frac{q^2}{\lambda}=2$ has been shown in [10].

for the δN with χ . From our estimation of Eq. (5.11) it comes out to be little higher than the slope in the lattice result of [10]. This is one of the main findings of our paper, that the curvature perturbation depends not only on the parametric resonance but also on the finer dynamics of preheating like rescattering and exact process responsible for the end of preheating.

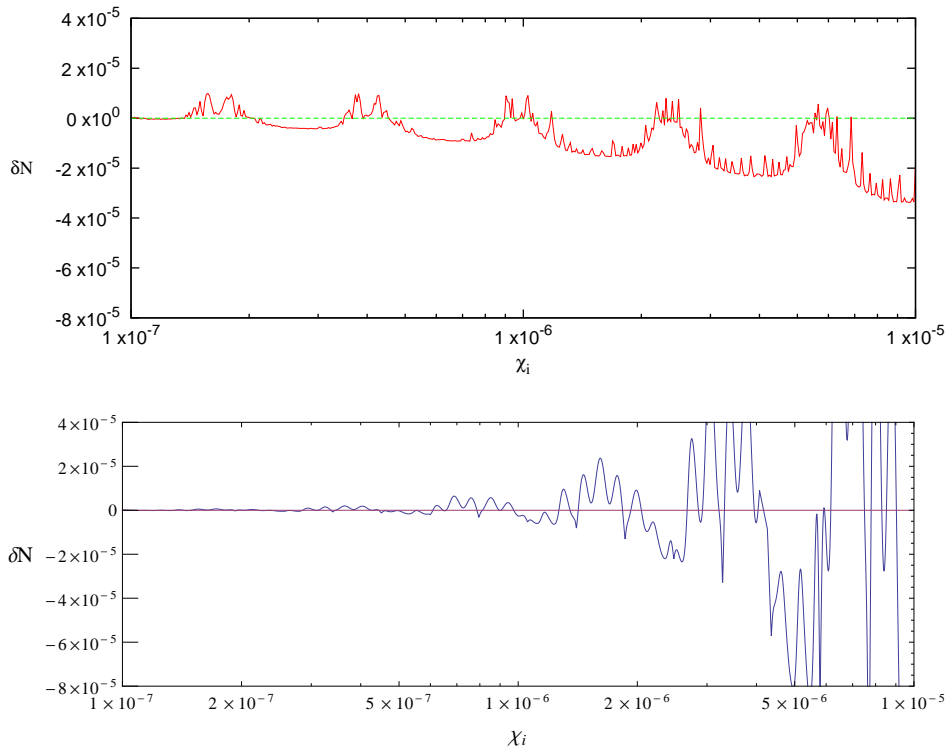


Figure 3. The upper panel shows lattice simulation of $\delta N(\chi_i)$ for $\frac{q^2}{\lambda^2}=200$. The lower panel shows the analytic result following from Eq. (4.6) for this parameter choice.

5.4 $\frac{q^2}{\lambda^2} = 200$ case

To double check if our formalism is right or wrong we do the lattice simulation for the same model with $\frac{q^2}{\lambda^2}=200$ in Fig. 3¹. Such a high value of $\frac{q^2}{\lambda^2}$ is irrelevant for the production of non-gaussianity in large scale. It makes χ field heavier than Hubble parameter during inflation and thus no super-horizon perturbation of χ gets produced. So applying δN formulation during preheating era becomes impossible.

The dynamics of χ_i is totally different in this case. For this value of $\frac{q^2}{\lambda^2}$ the $\kappa = 0$ mode doesn't get amplified, but the higher κ modes gets. Still they have quite small value of μ . So in the Fig. 4 we can see that $\langle X^2 \rangle$ initially grows slowly. The moment $\frac{\tilde{q}^2}{\lambda^2}$ reduces to 180 the $\kappa = 0$ mode starts increasing. At $\frac{\tilde{q}^2}{\lambda^2} = 178$ it gets its highest value $\mu = 0.23$. So we repeat the earlier formulation with this value of μ keep the assumed form of $X(\eta)$ as Eq. (5.1). There are few more things which gets modified in this $\frac{q^2}{\lambda^2} = 200$ case than the previous one. Firstly due to the change in ξ and $\frac{q^2}{\lambda^2}$ the value of $\langle X^2 \rangle_{\text{sat}}$ gets modified. It comes down to 0.01 and η_f^0 comes to be $\frac{48}{\sqrt{\lambda\Phi}}$. ω_Φ is 3ω . One can numerically find out that the value of n can be taken to be 7. n_Φ has been taken to be of the order of 10^6 .

Unlike the $\frac{q^2}{\lambda^2} = 2$ case, at the end of resonance X field gets a large non-oscillatory inhomogeneous $\langle \delta X^2 \rangle$, for both $\chi_i = 0$ and nonzero case. So in $\Delta\mathcal{H}_f$ there is non-oscillatory part. This part magnifies the effect of Lyapunov exponent in the plot of $\delta N(\chi)$ of Fig. 3. We see $\delta N(\chi_i)$ matches well with the lattice result. As the earlier case exact match can only be possible if the exact dynamics of rescattering

¹Lattice simulation is done using publicly available LatticeEasy code[43]. The default code cannot give energy conservation accuracy(ECA) less than 10^{-3} . We have achieved an ECA of order 10^{-7} reducing the time step and using double precision. The above plot is a result of simulations with 1000 different initial χ values on 32^3 lattice. Length of the lattice has been set at $20/H_e$, where H_e is the value of Hubble parameter at the end of inflation

and backreaction is understood.

So in short from the above discussions we understand that the spiky patterns are the manifestation of the increase in the frequency of the homogeneous mode of Φ at the final period of preheating. As the frequency becomes higher, the number of spikes increases. We also understand that the increase in the amplitude of δN with χ_i comes from the fact that the saturation value of X (X_{\max}) increases with the increase in χ_i . The dependence of X_{\max} on χ_i determines how δN would increase with χ_i . From some logical arguments developed following the line of [40], we got $X_{\max} = X_{\text{sat}} + \beta\chi_i^2$. But to exactly determine the dependency of X_{\max} on χ_i , one needs to study the rescattering of ϕ particles with the homogeneous condensate of χ particles. Since we have taken a χ_i^2 dependence of X_{\max} , we have got a suppressed value of δN for the lower values of χ_i and elevated values δN for larger χ_i . From the lattice simulation of [10] it seems that X_{\max} should depend on some lower power of χ_i than χ_i^2 because in that case spikes in the lower χ_i region will be more visible.

6 Non-gaussianity

In the second part of our paper we move on to calculate the effect of curvature perturbations on CMB, generated in preheating era. The exact functional form of the quantities shown in Fig. 2 is too much complicated to analytically predict the value of any observable quantity. So we pick out a few terms from the total expressions of Eq. (4.6) which are most dominating in yielding the shape of δN . After calculations those terms give the following simplified form of δN ,

$$\begin{aligned} \delta N(\chi_i) \approx & \frac{\sqrt{8\pi}}{2} C \left[\frac{\frac{g^2}{\lambda} \beta \Phi(\eta_f) \sqrt{\lambda(\Phi(\eta_f)^2 + 2\frac{g^2}{\lambda} X_{\text{sat}}^2)}}{2 \left(\Phi(\eta_f)^2 + 2\frac{g^2}{\lambda} X_{\text{sat}}^2 \right)^2} \chi_i^2 \right] \\ & \times \left(\frac{\left(\frac{47}{32} - \log 2 \right) \log \frac{X_{\text{sat}}}{\chi_i} - \frac{135}{1024} \frac{g^2}{\lambda} \frac{X_{\text{sat}}^2}{\tilde{\Phi}^2} \frac{\mu \cos \left(2 \log \frac{X_{\text{sat}}}{\chi_i} \right) + \sin \left(2 \log \frac{X_{\text{sat}}}{\chi_i} \right)}{(1 + \mu^2)\omega}}{\mu\omega} \right. \\ & \left. - \frac{27}{256} \frac{g^4}{\lambda^2} \frac{X_{\text{sat}}^4}{\tilde{\Phi}^4} \frac{2\mu \cos \left(2 \log \frac{X_{\text{sat}}}{\chi_i} \right) + \sin \left(2 \log \frac{X_{\text{sat}}}{\chi_i} \right)}{(1 + 4\mu^2)\omega} \right) \\ & - \left[\frac{\frac{g^2}{\lambda} \alpha \beta \left(-8 + 3C\sqrt{2\pi} \sqrt{\lambda\Phi(\eta_f)^2(\Phi(\eta_f)^2 + 2\frac{g^2}{\lambda} X_{\text{sat}}^2)} \left[\int e^{\Lambda\tau} d\tau \Big|_{\eta_f} \right]_{\text{avg}} \right)}{4(\Phi(\eta_f)^2 + 2\frac{g^2}{\lambda} X_{\text{sat}}^2)} \chi_i^2 \right]. \end{aligned} \quad (6.1)$$

This is the main result of our paper. In principle one can calculate the non-gaussianity parameters using this expression of δN . There are two methods for this purpose in literature. First one Fourier decomposes $\delta N(\chi_i)$ in terms of variance and then calculate the three point correlation function [13]. We have failed to use it for the $\delta N(\chi_i)$ of Eq. (6.1). So we follow the second method which has been described in section 3.

We smooth out Eq. (6.1) on the large scales by the gaussian window function as Eq. (3.3).

$$\delta N_R(\chi') = \int_{-\infty}^{\infty} \delta N(\chi) W_\chi(\chi' - \chi) d\chi = 2 \int_0^{\infty} \delta N(\chi) W_\chi(\chi' - \chi) d\chi. \quad (6.2)$$

The last step follows from the fact that $\delta N(\chi_i)$ depends only on the absolute value of χ_i . So, if we change the variable χ_i to $y = \log \chi_i$ then Eq. (6.2) gets the following form,

$$\delta N_R(\chi') = 2 \int_{-\infty}^{\infty} \delta N(y) \underbrace{\frac{e^y}{\sqrt{2\pi}\sigma} \exp\left(-\frac{(e^y - \chi')^2}{\sigma^2}\right)}_{W_y} dy. \quad (6.3)$$

For computing the integration of Eq. (6.3) analytically, we use the following method. We expand W_y in terms of a gaussian function G_y using Edgeworth expansion [44]

$$W_y(y, \chi') = G_y(y, y_0) \left[1 - K_1 \frac{y}{\gamma} + \frac{K_2}{2\gamma^2} \left(\frac{y^2}{\gamma^2} - 1 \right) - \frac{K_3}{6\gamma^3} \left(\frac{y^3}{\gamma^3} - 3\frac{y}{\gamma} \right) + \dots \right], \quad (6.4)$$

where

$$G_y(y, y_0) = \frac{1}{\sqrt{2\pi}\gamma} \exp - \left(\frac{y - y_0}{\sqrt{2}\gamma} \right)^2. \quad (6.5)$$

Here K_i, y_0 and γ are functions of σ and χ' (see Appendix C). y_0 is the value of y for which W_y becomes maximum. So, y_0 is not necessarily the mean value of the distribution. The coefficient K_1 takes care of the shift in the mean. Similarly K_2 and K_3 take care of the change in variance and skewness. For the values of model parameters we have taken, σ gets a value of 8.38×10^{-8} . This expansion fits quite well for $\chi' > 5 \times 10^{-8}$. So whatever result we would obtain after integrating Eq. (6.3) is valid for such a choice of χ' .

After changing the variable to y we get four types of terms. The contribution of the terms $e^{2y} \sin ny$ and $e^{2y} y \sin ny$ are proportional to $e^{2-\frac{n^2}{2}+2y_0} \sin[n(2+y_0)]$ after performing the integration Eq. (6.3). Thus for large values of χ_i when y_0 is quite small, we can expect that the low frequency modulation contributes in the smoothed out δN_R . This can be seen in the numerical integration performed in [10]. We are not interested in such high values of χ_i . Therefore we are interested only in these two types of terms which are proportional to e^{2y} and $e^{2y} y$.

After doing the integration of Eq. (6.3) using Eq. (6.1) we find $\delta N_R(\chi')$ takes the following form,

$$\delta N_R(\chi') \approx e^{2(y_0+\gamma^2)} \sqrt{\gamma} [C_1 + C_2(y_0 + 2\gamma^2)], \quad (6.6)$$

where the exact expressions of C_1 and C_2 are shown in Appendix C. For more accurate determination of δN_R higher order terms like K_3 or K_4 can be taken into consideration. But the form of Eq. (6.6) remains same. Expanding Eq. (6.6) in a converging series of χ' as Eq. (1.1) or Eq. (3.4) is impossible for the large range of χ' . The reason behind this is that γ, y_0 and C_1, C_2 can not be expanded in converging series of χ' . Still we find that the dependence of δN_R on χ' is mostly proportional to $|\chi'|$. We don't know what kind of signature it would produce in non-gaussianity parameters. Still to have an idea of the order of f_{NL} we write approximately Eq. (6.6) in a small range of $7 \times 10^{-8} < \chi' < 3 \times 10^{-7}$ as

$$\delta N_R(\chi') \approx 10^9 \chi'^2. \quad (6.7)$$

Using the second term of Eq. (3.8) we get $F_{NL}^{\text{local}} \sim \mathcal{O}(1)$. We have used $P_\chi \sim 2 \times 10^{-15}$ and $P_\zeta \approx 2.4 \times 10^{-9}$.

But as discussed earlier the value of F_{NL} can vary depending on the range of χ' . So, this result does not in any sense mean to be taken as prediction of F_{NL} .

7 Conclusion

In this work we have developed a technique for calculating curvature perturbation in the era of preheating. During this era, different disconnected Hubble patches evolve differently. We have used Lyapunov theorem to calculate the separation between different evolution trajectories of Hubble parameters. This method has enabled us to use δN formulation and calculate a functional form of curvature perturbation analytically. In this way we have been able to establish a one-to-one connection between the finer dynamics of preheating and the super-horizon curvature perturbation. We have shown the dependency of saturation value of the secondary field, χ with its initial background value plays a crucial role in the expression of curvature perturbation or δN .

The parametric resonance of χ ends via different dynamics for different models of potentials. In some cases rescattering produces enough amount of inflaton particles and forces the parametric resonance to shut down. In other models restructuring of resonance might play the role. But availability of background field value of χ can act as a homogeneous condensate of χ particles and might effect the process of rescattering. Similarly, change in inflaton particle production can alter the production of χ particles just after the end of the parametric resonance. These dynamics changes the saturation value of χ (X_{\max}) for its different initial background values (χ_i). Detailed calculation of how X_{\max} depends on χ_i has not been explored in previous literatures. We have shown that this relation is the most important factor for the determination of $\delta N(\chi_i)$.

Here we have calculated a relation between X_{\max} and χ_i from some simple logical arguments. Using that we have presented a simplified and approximated form of $\delta N(\chi_i)$. This form matches quite well with the shape of $\delta N(\chi_i)$ computed using lattice simulation [10]. To check whether our formulation is correct or not, we have performed lattice simulation for another set of parameter values and we have observed that it matches reasonably well with the analytical calculation. The lattice results indicate that the relation between X_{\max} and χ_i needs to be modified to have an exact match. So future works are required in this direction.

The second problem we have attempted to solve is how the curvature perturbation δN produced in era of preheating can show up in large scales of CMB. From the functional form of $\delta N(\chi_i)$ we see that it depends on $\log \chi_i$ that means as expected earlier by various authors δN would depend only on the absolute value of χ_i . We smooth out the $\delta N(\chi_i)$ with suitable Gaussian window function and we have given an analytical form of curvature perturbation smoothed out on large scales (δN_R). This δN_R cannot be expanded in a converging series of χ for the entire range. Therefore as expected by earlier authors to approximate δN_R as a quadratic function of χ for any arbitrary values of χ . Although we have taken an approximate quadratic form of δN_R to have an estimation of the order of local form non-gaussianity parameter F_{NL} , this estimation might not hold for any arbitrary values of χ_i . So, we restrict ourselves from predicting any particular value of non-gaussianity parameter F_{NL} . Rather we pose it as a problem to be addressed for the cases where δN_R depends on $\log \chi$.

Therefore in total we have built a formulation for calculating curvature perturbation from the dynamics of preheating and we have methodically shown how some specific quantity of preheating dynamics effects different features of δN . We have taken the massless preheating model just to have a comparison with the available lattice simulation in the literature. But, in general, the procedure developed here for calculating $\delta N(\chi)$ can be applicable to any other potentials. Even for this potential one can incorporate the contribution of more finer dynamics like the oscillation of inhomogeneous modes of inflaton and see its effect on $\delta N(\chi)$. Therefore we hope that our study would serve as a good platform for accurate determination of f_{NL} from preheating in future.

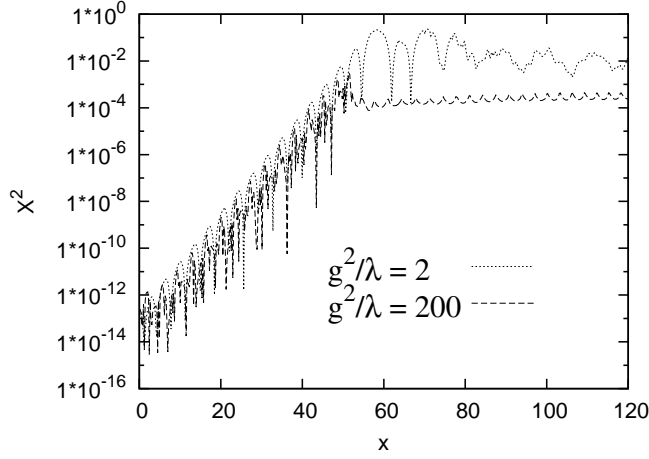


Figure 4. Growth of the field X^2 for different values of $\frac{g^2}{\lambda}$. Here $x = \sqrt{\lambda}\tilde{\Phi}\eta$ as described in section 2

Appendix

A Calculation for node shift dependence of $\Delta\mathcal{H}$

Using Eq. (4.9) we expand the difference between two solutions of \mathcal{H} with different initial condition with respect to their initial difference $\Delta\mathcal{H}_i$ and take up to the first order term.

$$\Delta\mathcal{H}(\tau) = \mathcal{H}(\tau, \mathcal{H}_i + \Delta\mathcal{H}_i) - \mathcal{H}(\tau, \Delta\mathcal{H}_i) = \frac{A^2}{(A \cosh(A\tau) + \mathcal{H}_i \sinh(A\tau))^2} \Delta\mathcal{H}_i \quad (\text{A.1})$$

So

$$B = \frac{A}{(A \cosh(A\tau) + \mathcal{H}_i \sinh(A\tau))^2} \quad (\text{A.2})$$

Now by introducing the change in A we come up to Eq. (4.14) where the function C is

$$C(\mathcal{H}_i, \tau, A) = \frac{1}{4A^2} e^{2A\tau} (\mathcal{H}_i + e^{-2A\tau}\mathcal{H}_i + A - Ae^{-2A\tau}) (\mathcal{H}_i - e^{-2A\tau}\mathcal{H}_i + A + Ae^{-2A\tau}) \quad (\text{A.3})$$

If write $A = 8\pi\mathcal{V}$ and τ at the end of the preheating is of the order of $\mathcal{O}(10^2)\eta_f$ and $\mathcal{H}_i = \frac{\lambda}{4}\tilde{\Phi}^4$ we get $C \approx \mathcal{O}(1)$.

B Determination of the necessary quantities

We determine two quantities for the evaluation of Eq. (5.6) and Eq. (5.11) from lattice simulation results using [43]. First one is the co-moving time η_f^0 when the X reaches its saturation value for $\chi_i = 0$ case, and second one is the value of X field at saturation level called X_{sat} . In the Fig. B the growth of the X field with $\sqrt{\lambda}\tilde{\Phi}\eta$ has been shown for different values of $\frac{g^2}{\lambda}$. For both the case χ_i has been taken to be zero. The maximum value reached by X is recorded as X_{sat} , and corresponding co-moving time as η_f^0 . X_{max} in the Eq. (5.11) is this maximum value of X for nonzero χ_i cases. From the plots we get X_{sat}^2 to be 0.39 and $\eta_f^0 = \frac{59}{\sqrt{\lambda}\tilde{\Phi}}$ for $\frac{g^2}{\lambda} = 2$. For $\frac{g^2}{\lambda} = 200$, X_{sat}^2 turns out to be and 10^{-4} and η_f^0 to be $\frac{48}{\sqrt{\lambda}\tilde{\Phi}}$.

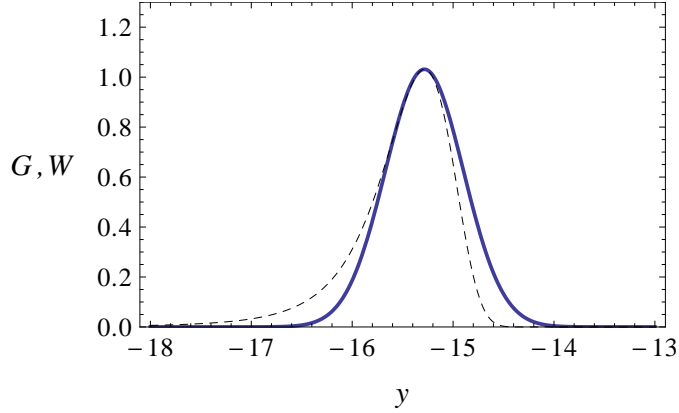


Figure 5. Probability distribution functions (G and W) for $\log(x) = y$ with $\sigma = 8.38 \times 10^{-8}$ and $\chi' = 2 \times 10^{-7}$. G_y has been shown with solid line and W_y by dashed line. This indicates that slightly non-gaussian W_y can be expanded in terms of fully gaussian G_y .

C Expansion of W_y

Edgeworth expansion is an expansion of slightly non-gaussian probability distribution function in a polynomial series multiplied by a gaussian function as shown in Eq. (6.4). First thing one need to do is to fix a suitable gaussian function so that the error can be minimized. We choose the mean value (y_0) of the gaussian function G_y to be that value of y for which W_y reaches maximum. So, y_0 turns out to be

$$y_0 = \log \left[\frac{1}{2} \left(\chi' + \sqrt{4\sigma^2 + \chi'^2} \right) \right]. \quad (\text{C.1})$$

Second thing to be fixed is the variance γ . To fix this we choose the height of the G_y and the W_y to be equal, which gives

$$\gamma^{-1} = \frac{1}{2\sigma} \left(\chi' + \sqrt{4\sigma^2 + \chi'^2} \right) \exp \left[\frac{\left(-\chi' + \frac{1}{2} \left(\chi' + \sqrt{4\sigma^2 + \chi'^2} \right) \right)^2}{2\sigma^2} \right] \quad (\text{C.2})$$

It can be an interesting matter of study that which choice of γ and y_0 can give best fit up to a certain order of expansion, and how does the value of f_{NL} depends on this choice. For this present paper we avoid this discussion. But just for an illustration we plot the W_y and the G_y in Fig. 5 with some realistic values of σ and χ' . Now we move on to calculate K_i s. K_1 is defined as

$$\begin{aligned} K_1 &= \int_{-\infty}^{\infty} \left(\frac{y - y_0}{\gamma} \right) W_y = \int_0^{\infty} \left(\frac{\log x - y_0}{\gamma} \right) \frac{1}{\sqrt{2\pi}\sigma} e^{-\frac{(x-\chi')^2}{2\sigma^2}} \\ &= \frac{1}{4\sigma\gamma} e^{-\frac{\chi'^2}{2\sigma^2}} \left\{ -e^{\frac{\chi'^2}{2\sigma^2}} \sigma \left(\gamma_E + 2y_0 + \log 2 + \text{Erf} \left[\frac{\chi'}{\sqrt{2}\sigma} \right] \left(\gamma_E + 2y_0 + \log \frac{1}{2\sigma^2} \right) - 2 \log \sigma \right. \right. \\ &\quad \left. \left. + \text{F}_1 \left[0, \frac{1}{2}, -\frac{\chi'^2}{2\sigma^2} \right] \right) + \sqrt{\frac{2}{\pi}} \chi' \text{F}_1 \left[1, \frac{3}{2}, \frac{\chi'^2}{2\sigma^2} \right] \right\} \quad (\text{C.3}) \end{aligned}$$

Here F_1 is the hyper-geometric function of first kind. γ_E is the Euler gamma which has a value of 0.577.

K_2 is defined as follows

$$K_2 = \int_{-\infty}^{\infty} \left(\left(\frac{y - y_0}{\gamma} \right)^2 - 1 \right) W_y = \int_0^{\infty} \left(\left(\frac{\log x - y_0}{\gamma} \right)^2 - 1 \right) \frac{1}{\sqrt{2\pi}\sigma} e^{-\frac{(x-\chi')^2}{2\sigma^2}} \quad (\text{C.4})$$

For analytically performing this integration we expand $\log \chi$ in terms of $\frac{\chi}{2\sigma}$ as,

$$\log \chi = \log \frac{\chi}{2\sigma} + \log(2\sigma) = -\frac{3}{2} + \frac{\chi}{\sigma} - \frac{\chi^2}{8\sigma^2} + \log(2\sigma). \quad (\text{C.5})$$

Using this we get,

$$\begin{aligned} K_2 = & \frac{1}{128\sqrt{2\pi}\gamma^2\sigma^4\chi'} e^{-\frac{\chi'^2}{2\sigma^2}} \left[\chi' \left\{ \left(-64(7 + 4y_0) + e^{\frac{\chi'^2}{2\sigma^2}} \sqrt{2\pi}(235 + 208y_0 + 64y_0^2 - 64\gamma^2) \right) \sigma^4 - \right. \right. \\ & 2 \left(-93 - 16y_0 + 8e^{\frac{\chi'^2}{2\sigma^2}} \sqrt{2\pi}(15 + 8y_0) \right) \sigma^3 \chi' + 2 \left(-16 + e^{\frac{\chi'^2}{2\sigma^2}} \sqrt{2\pi}(47 + 8y_0) \right) \sigma^2 \chi'^2 - \\ & 2 \left(-1 + 8e^{\frac{\chi'^2}{2\sigma^2}} \sqrt{2\pi} \right) \sigma \chi'^3 + e^{\frac{\chi'^2}{2\sigma^2}} \sqrt{2\pi} \chi'^4 \left. \right\} + e^{\frac{\chi'^2}{2\sigma^2}} \sqrt{2\pi} \chi' \left((235 + 208y_0 + 64y_0^2 - 64\gamma^2) \sigma^4 - \right. \\ & 16(15 + 8y_0) \sigma^3 \chi' + 2(47 + 8y_0) \sigma^2 \chi'^2 - 16\sigma \chi'^3 + \chi'^4 \left. \right) \text{Erf} \left[\frac{\chi'}{\sqrt{2}\sigma} \right] - \\ & 16\sigma^2 \left\{ \chi' \left((-16 + e^{\frac{\chi'^2}{2\sigma^2}} \sqrt{2\pi}(13 + 8y_0)) \sigma^2 - 2(-1 + 4e^{\frac{\chi'^2}{2\sigma^2}} \sqrt{2\pi}) \sigma \chi' + e^{\frac{\chi'^2}{2\sigma^2}} \sqrt{2\pi} \chi'^2 \right) + \right. \\ & e^{\frac{\chi'^2}{2\sigma^2}} \sqrt{2\pi} \chi' \left((13 + 8y_0) \sigma^2 - 8\sigma \chi' + \chi'^2 \right) \text{Erf} \left[\frac{\chi'}{\sqrt{2}\sigma} \right] \left. \right\} \log[2\sigma] + \\ & \left. 64e^{\frac{\chi'^2}{2\sigma^2}} \sqrt{2\pi} \sigma^4 \left(\chi' + \chi' \text{Erf} \left[\frac{\chi'}{\sqrt{2}\sigma} \right] \right) \log[2\sigma]^2 \right] \quad (\text{C.6}) \end{aligned}$$

For $\sigma = 8.38 \times 10^{-8}$ the value of K_1 can be approximated as $-0.458 + 4.15 \times 10^{12} \chi'^2$ and the value of K_2 can be approximated as $-0.461 + 1.6 \times 10^{13} \chi'^2$. In the integration of $\delta N(\chi_i)$ (see Eq. (6.6)), for $\frac{q^2}{\chi} = 2$ case, we have

$$\begin{aligned} C_1 = & -3.96 \times 10^4 \left(1 + \frac{K_1 y_0}{\gamma} + \frac{K_2 y_0^2}{2\gamma^4} - \frac{K_2}{2\gamma^2} \right), \\ C_2 = & -1.28 \times 10^4 \left(1 + \frac{K_1 y_0}{\gamma} + \frac{K_2 y_0^2}{2\gamma^4} - \frac{K_2}{2\gamma^2} \right) + 3.96 \times 10^4 \left(\frac{K_1}{\gamma} + \frac{K_2 y_0}{\gamma^4} \right). \quad (\text{C.7}) \end{aligned}$$

Acknowledgement

We would like to thank Gary Felder for some discussions regarding LATTICEASY code. AM would like to acknowledge Palash B. Pal for fruitful suggestions in deriving the effect of node shift on Lyapunov theorem. The authors are thankful to Koushik Dutta and Palash B. Pal for helping in preparation of this manuscript. The authors acknowledge the Department of Atomic Energy (DAE, Govt. of India) for financial assistance.

References

- [1] K. Enqvist, A. Jokinen, A. Mazumdar, T. Multamaki, and A. Vaihkonen, *Non-Gaussianity from instant and tachyonic preheating*, *JCAP* **0503** (2005) 010, [[hep-ph/0501076](#)].
- [2] K. Enqvist, A. Jokinen, A. Mazumdar, T. Multamaki, and A. Vaihkonen, *Non-Gaussianity from preheating*, *Phys.Rev.Lett.* **94** (2005) 161301, [[astro-ph/0411394](#)].

- [3] N. Bartolo, S. Matarrese, and A. Riotto, *Enhancement of non-Gaussianity after inflation*, *JHEP* **0404** (2004) 006, [[astro-ph/0308088](#)].
- [4] K. Kohri, D. H. Lyth, and C. A. Valenzuela-Toledo, *Preheating and the non-gaussianity of the curvature perturbation*, *JCAP* **1002** (2010) 023, [[arXiv:0904.0793](#)].
- [5] A. Chambers and A. Rajantie, *Non-Gaussianity from massless preheating*, *JCAP* **0808** (2008) 002, [[arXiv:0805.4795](#)].
- [6] A. Chambers and A. Rajantie, *Lattice calculation of non-Gaussianity from preheating*, *Phys.Rev.Lett.* **100** (2008) 041302, [[arXiv:0710.4133](#)].
- [7] A. Jokinen and A. Mazumdar, *Very large primordial non-gaussianity from multi-field: application to massless preheating*, *JCAP* **0604** (2006) 003, [[astro-ph/0512368](#)].
- [8] C. T. Byrnes, *Constraints on generating the primordial curvature perturbation and non-Gaussianity from instant preheating*, *JCAP* **0901** (2009) 011, [[arXiv:0810.3913](#)].
- [9] A. R. Liddle, D. H. Lyth, K. A. Malik, and D. Wands, *Superhorizon perturbations and preheating*, *Phys.Rev.* **D61** (2000) 103509, [[hep-ph/9912473](#)].
- [10] J. R. Bond, A. V. Frolov, Z. Huang, and L. Kofman, *Non-Gaussian Spikes from Chaotic Billiards in Inflation Preheating*, *Phys.Rev.Lett.* **103** (2009) 071301, [[arXiv:0903.3407](#)].
- [11] A. V. Frolov, *Non-linear Dynamics and Primordial Curvature Perturbations from Preheating*, *Class.Quant.Grav.* **27** (2010) 124006, [[arXiv:1004.3559](#)].
- [12] L. Ackerman, C. W. Bauer, M. L. Graesser, and M. B. Wise, *Light scalars and the generation of density perturbations during preheating or inflaton decay*, *Phys.Lett.* **B611** (2005) 53–59, [[astro-ph/0412007](#)].
- [13] T. Suyama and S. Yokoyama, *Statistics of general functions of a Gaussian field-application to non-Gaussianity from preheating*, *JCAP* **1306** (2013) 018, [[arXiv:1303.1254](#)].
- [14] T. Hamazaki and H. Kodama, *Evolution of cosmological perturbations during reheating*, *Prog.Theor.Phys.* **96** (1996) 1123–1146, [[gr-qc/9609036](#)].
- [15] B. A. Bassett and F. Viniegra, *Massless metric preheating*, *Phys.Rev.* **D62** (2000) 043507, [[hep-ph/9909353](#)].
- [16] F. Finelli and R. H. Brandenberger, *Parametric amplification of metric fluctuations during reheating in two field models*, *Phys.Rev.* **D62** (2000) 083502, [[hep-ph/0003172](#)].
- [17] J. Zibin, R. H. Brandenberger, and D. Scott, *Back reaction and the parametric resonance of cosmological fluctuations*, *Phys.Rev.* **D63** (2001) 043511, [[hep-ph/0007219](#)].
- [18] M. Bruni, S. Matarrese, S. Mollerach, and S. Sonogo, *Perturbations of space-time: Gauge transformations and gauge invariance at second order and beyond*, *Class.Quant.Grav.* **14** (1997) 2585–2606, [[gr-qc/9609040](#)].
- [19] A. J. Christopherson, E. Nalson, and K. A. Malik, *A short note on the curvature perturbation at second order*, [arXiv:1409.5106](#).
- [20] M. Dias, J. Elliston, J. Frazer, D. Mulryne, and D. Seery, *The curvature perturbation at second order*, [arXiv:1410.3491](#).
- [21] H. B. Moghaddam, R. H. Brandenberger, Y.-F. Cai, and E. G. M. Ferreira, *Parametric Resonance of Entropy Perturbations in Massless Preheating*, [arXiv:1409.1784](#).
- [22] T. Tanaka and B. Bassett, *Application of the separate universe approach to preheating*, [astro-ph/0302544](#).
- [23] T. Suyama and S. Yokoyama, *Generating the primordial curvature perturbations in preheating*, *Class.Quant.Grav.* **24** (2007) 1615–1626, [[astro-ph/0606228](#)].
- [24] N. S. Sugiyama, E. Komatsu, and T. Futamase, *The δN Formalism*, *Phys.Rev.* **D87** (2013) 023530, [[arXiv:1208.1073](#)].
- [25] D. H. Lyth, K. A. Malik, and M. Sasaki, *A General proof of the conservation of the curvature perturbation*, *JCAP* **0505** (2005) 004, [[astro-ph/0411220](#)].

- [26] D. H. Lyth and Y. Rodriguez, *The Inflationary prediction for primordial non-Gaussianity*, *Phys.Rev.Lett.* **95** (2005) 121302, [[astro-ph/0504045](#)].
- [27] **Planck Collaboration** Collaboration, P. Ade et al., *Planck 2013 Results. XXIV. Constraints on primordial non-Gaussianity*, [arXiv:1303.5084](#).
- [28] **Planck** Collaboration, P. Ade et al., *Planck 2013 results. XXII. Constraints on inflation*, *Astron.Astrophys.* **571** (2014) A22, [[arXiv:1303.5082](#)].
- [29] G. N. Felder, L. Kofman, and A. D. Linde, *Tachyonic instability and dynamics of spontaneous symmetry breaking*, *Phys.Rev.* **D64** (2001) 123517, [[hep-th/0106179](#)].
- [30] P. B. Greene, L. Kofman, A. D. Linde, and A. A. Starobinsky, *Structure of resonance in preheating after inflation*, *Phys.Rev.* **D56** (1997) 6175–6192, [[hep-ph/9705347](#)].
- [31] D. H. Lyth, *Generating the curvature perturbation at the end of inflation*, *JCAP* **0511** (2005) 006, [[astro-ph/0510443](#)].
- [32] L. Boubekeur and D. Lyth, *Detecting a small perturbation through its non-Gaussianity*, *Phys.Rev.* **D73** (2006) 021301, [[astro-ph/0504046](#)].
- [33] D. H. Lyth and Y. Rodriguez, *Non-Gaussianity from the second-order cosmological perturbation*, *Phys.Rev.* **D71** (2005) 123508, [[astro-ph/0502578](#)].
- [34] E. Komatsu, *The pursuit of non-gaussian fluctuations in the cosmic microwave background*, [astro-ph/0206039](#).
- [35] N. Bartolo, E. Komatsu, S. Matarrese, and A. Riotto, *Non-Gaussianity from inflation: Theory and observations*, *Phys.Rept.* **402** (2004) 103–266, [[astro-ph/0406398](#)].
- [36] M. Liguori, F. Hansen, E. Komatsu, S. Matarrese, and A. Riotto, *Testing primordial non-gaussianity in cmb anisotropies*, *Phys.Rev.* **D73** (2006) 043505, [[astro-ph/0509098](#)].
- [37] D. I. Podolsky, G. N. Felder, L. Kofman, and M. Peloso, *Equation of state and beginning of thermalization after preheating*, *Phys.Rev.* **D73** (2006) 023501, [[hep-ph/0507096](#)].
- [38] G. B. Arfken and H. J. Weber, *Mathematical methods for physicists* . (2005).
- [39] S. H. Strogatz, *Nonlinear dynamics and chaos*, Westview Press (1994).
- [40] L. Kofman, A. D. Linde, and A. A. Starobinsky, *Towards the theory of reheating after inflation*, *Phys.Rev.* **D56** (1997) 3258–3295, [[hep-ph/9704452](#)].
- [41] S. Y. Khlebnikov and I. Tkachev, *Classical decay of inflaton*, *Phys.Rev.Lett.* **77** (1996) 219–222, [[hep-ph/9603378](#)].
- [42] S. Y. Khlebnikov and I. Tkachev, *Resonant decay of Bose condensates*, *Phys.Rev.Lett.* **79** (1997) 1607–1610, [[hep-ph/9610477](#)].
- [43] G. N. Felder and I. Tkachev, *LATTICEEASY: A Program for lattice simulations of scalar fields in an expanding universe*, *Comput.Phys.Commun.* **178** (2008) 929–932, [[hep-ph/0011159](#)].
- [44] F. Bernardeau and L. Kofman, *Properties of the cosmological density distribution function*, *Astrophys.J.* **443** (1995) 479–498, [[astro-ph/9403028](#)].